ELSEVIER

Journal of Nuclear Materials 290–293 (2001) 668–672

journal of nuclear materials

www.elsevier.nl/locate/jnucmat

Divertor energy distribution in JET H-modes

G.F. Matthews [a,b,*], S.K. Erents [a,b], W. Fundamenski [a,b], C. Ingesson [a,c], R.D. Monk [a,d], V. Riccardo [a,b]

[a] JET Joint Undertaking, Abingdon, Oxfordshire OX 14 3EA, UK
[b] UKAEA Fusion, Culham Science Centre, Abingdon, Oxfordshire OX14 3EA,UK
[c] FOM Instituut voor Plasmafysica Rijnhuizen, EURATOM Association, Postbus 1207, NL-3430 BE Nieuwegein, Netherlands
[d] Max-Planck-Institut für Plasmaphysik, IPP-EURATOM Association, Boltzmannstrasse 2, D-85748, Germany

Abstract

Divertor tile calorimetry is shown to provide accurate routine energy balance in JET. By shifting the plasma from pulse-to-pulse a power profile is reconstructed which shows a narrow high power peak at the outer target, 2 mm mid-plane in width. This feature carries half the total divertor power in a typical type I ELMy H-mode and is the dominant factor determining the in/out divertor energy asymmetry. © 2001 JET Joint Undertaking. Published by Elsevier Science B.V. All rights reserved.

Keywords: Divertor; Energy balance; Calorimetry; Target profiles

1. Introduction

Despite extensive studies of the power deposition profiles in JET using fast IR cameras and target Langmuir probes, significant uncertainties have remained about the power deposition profiles in ELMy H-modes. Fast IR data appear to be confused by the presence of thermally detached surface layers [1,2]. ELM power flow, determined by fast diamagnetic measurements, corresponds to up to 20% of the input power and 30% of the power flow to the divertor. Target Langmuir probe analysis only gives reliable profiles in the inter-ELM periods and can only determine the power flow in the electron channel. We show in this paper that the JET tile thermocouples, although poor in time resolution, provide accurate measurements of the energy distribution in the JET divertor.

2. Tile calorimetry

The tiles in the JET MkIIa and MkIIGB divertors are thermally isolated from the support structure and cool radiatively after each pulse with a time constant of order 1000 s. Fig. 1 includes a schematic showing the location of the tile thermocouples in the MkIIGB divertor. In MkIIa the thermocouples were pressed on the back of each tile whilst in MkIIGB the thermocouples were inserted into within 1 cm of the tile surface and there were more than one thermocouple per tile. After each pulse the thermocouple data are collected for a period of around 1200 s. Fig. 1 shows the typical data from the inner and outer vertical tiles of MkIIGB for an ELMy H-mode pulse heated with 12 MW of neutral beams.

There are two thermocouples in each tile and during the pulse the thermocouple nearest to the strike point shows the greatest temperature rise while that further away rises more slowly as the heat is redistributed within the tile. After 500 s the tiles have more or less reached internal thermal equilibrium. The procedure adopted is to average together the two tile thermocouples after 500 s and fit a radiation cooling curve from the numerical integration of:

$$\frac{dT_{TC}}{dt} = a(T_0^4 - T_{TC}^4),$$

where T_{TC} is the thermocouple temperature in °K, T_0 the temperature of the radiation sink and a is a constant. Both a and T_0 are determined from the non-linear least

* Corresponding author. Tel.: +44-1235 464523; fax: +44-1235 464766.
E-mail address: gfm@jet.uk (G.F. Matthews).

PII: S0022-3115(00)00482-7

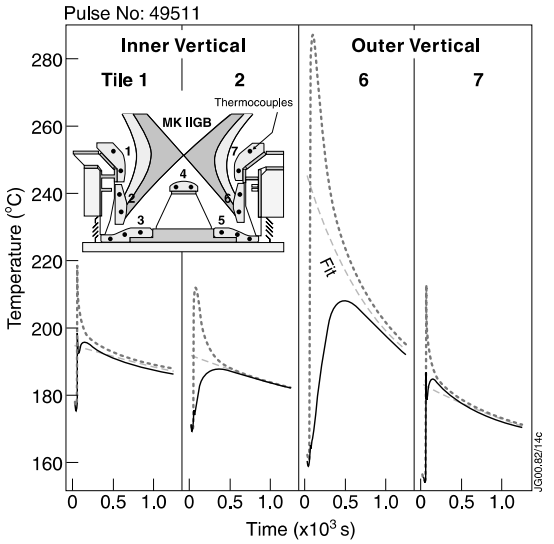

Fig. 1. Long-term thermal response of inner and outer vertical MkIIGB tiles following a typical 12 MW ELMy H-mode pulse. A radiation cooling curve is fitted after 500 s and extrapolated back to the end of the pulse.

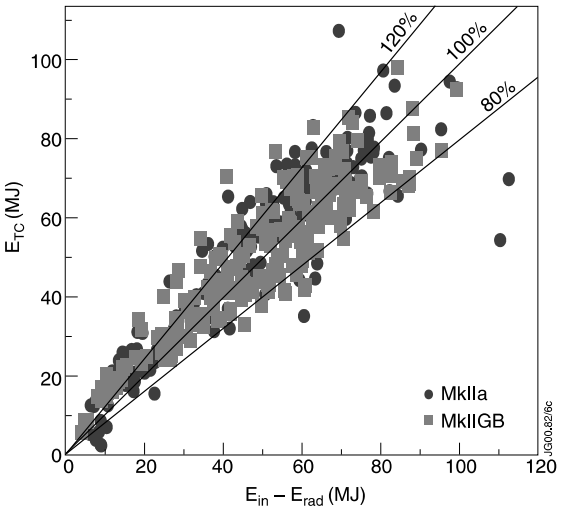

Fig. 2. Measured, E_{TC}, and expected $E_{in} - E_{rad}$ energies for all pulses in the JET steady-state database for MkIIa and MkIIGB.

squares fitting procedure. Having determined these constants the cooling curve for the tile at a single uniform temperature is back extrapolated to the end of the heating pulse. This gives us a bulk tile temperature rise for the whole pulse which combined with the temperature-dependent specific heat data and tile mass is used to calculate the tile energy. However, it must be pointed out that this procedure is not rigorous when the tiles are out of the internal thermal equilibrium but has been found to produce low scatter in the resulting energy balance.

3. Global energy balance

Fig. 2 shows the total divertor energy determined from tile thermocouples E_{TC} plotted against that which would be expected from the difference between the energy input, E_{in}, minus the radiated energy, E_{rad}, calculated for the divertor phase of each discharge. The database covers a wide range of equilibria and plasma conditions including low and high triangularity discharges, impurity seeded H-modes and pulses with RF heating. Despite this range almost all the data fall within $\pm 20\%$ of the expected value. Uncertainties in the total input power and radiated power are of the order of 10%.

The radiated energy comes from integration of main chamber bolometer data and no account is taken of the radiation falling on the divertor, amounting to $\sim 10\%$ of the total. It turns out however, that this omission is just sufficient to offset an underestimate ($\sim 10\%$) in the total radiated power as deduced from full tomographic reconstructions of the data [3].

The pulse-to-pulse reproducibility of the energy balance is higher than for the database as a whole, a few percent error is typical. Fig. 3 shows a plot of the global energy balance for a more restricted set of L and H-mode data. The purpose is to see whether there is a systematic difference in the energy balance between L

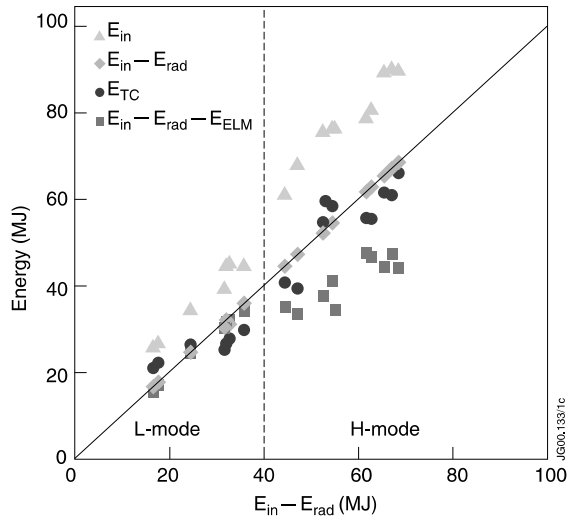

Fig. 3. Measured, E_{TC}, and expected $E_{in} - E_{rad}$ energies for selected L and H-mode pulses. Also shown is the predicted energy balance if all the ELM energy were deposited outside of the divertor.

and H-mode which might be expected if a significant fraction of the ELM energy went to the walls rather than the divertor. The ELM energy is defined by: $E_{ELM} = \Delta W_{dia} f_{ELM} t_{heat}$, where ΔW_{dia} is the average energy drop per ELM as determined by the fast diamagnetic loop, f_{ELM} the average ELM frequency and t_{heat} is the duration of heating pulse for which ELMs are present. If all the ELM energy went to the walls then we would expect that $E_{TC} = E_{in} - E_{rad} - E_{ELM}$. In Fig. 3 one can see that the thermocouple data are most consistent with a majority of the ELM energy going to the divertor, i.e. $E_{TC} = E_{in} - E_{rad}$. Given the possible absolute errors however the more significant result is that there is no change in energy accountability between L and H-modes.

4. Energy distribution

Fig. 4 shows an example of the individual tile energies from a typical ELMy H-mode in MkIIGB. In addition to the individual tile energies, this figure also shows the E_{in} and $E_{in} - E_{rad}$ which is in good agreement with E_{TC}.

Two features of Fig. 4 are worthy of note: The first is the large asymmetry between the inner and outer divertors which is typical of JET H-modes. The second is the small but real amount of energy recorded by tiles 3, 4 (septum) and 5 which is due to electromagnetic plasma radiation and bombardment by neutral particles. Averaged over the surface area of each tile, in the case of pulse 49511 the surface power density due to these sources is: 0.12 MW m^{-2} on inner horizontal tile 3, 0.16

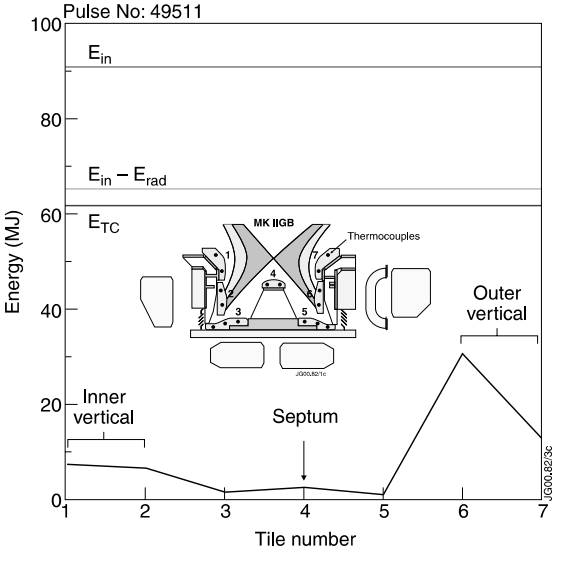

Fig. 4. Distribution of energy between tiles in MkIIGB for a typical ELMy H-mode.

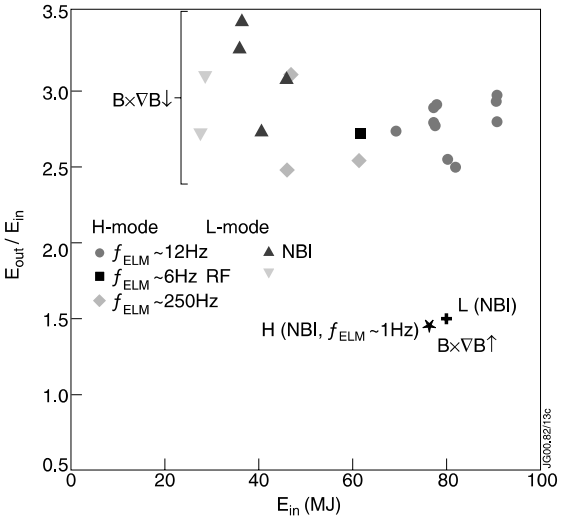

Fig. 5. Outer to inner divertor energy ratio vs input energy.

MW m^{-2} on the septum and 0.07 MW m^{-2} on outer horizontal tile 5. In Fig. 5 the outer to inner energy ratio is plotted for a similar set of discharges at 2.5 MA/2.5 T with vertical low triangularity configurations. Pulses are categorised according to the ELM frequency and confinement mode. Also compared are pulses with the $\mathbf{B} \times \nabla \mathbf{B}$ drift towards ↓ and away ↑ from the X-point.

The results of Fig. 5 show that the in/out energy asymmetry does not change significantly with ELM frequency from zero (L-mode) to 12 Hz (type I ELMs) to 250 Hz (type III ELMs). E_{outer}/E_{inner} is quite sensitive to the in/out distribution of the ELM energy because the total energy arriving at the inner target is comparable to the ELM energy. These results imply that the ELM energy is split between outer and inner divertors in a similar ratio i.e. 3:1 or that the power is even more asymmetric in favour of the outside during inter-ELM periods than in L-mode.

5. Power profile determination

A dedicated series of pulses was carried out in which a high clearance plasma configuration was shifted vertically up the divertor target on a pulse-to-pulse basis. The pulses were all standard ELMy H-modes ($I_p = 2.5$ MA, $B_T = 2.5$ T, $P_{NBI} = 12$ MW, $f_{ELM} \sim 10$ Hz) and were unaffected by the change in vertical position. Since the energy input is not exactly the same in all pulses, the fraction of the energy going to each lower vertical tile is normalised to the total energy measured on both inner and outer vertical tiles. Hence, the fractional energy deposited on tile 6 is F6 = (E6/(E6 + E7)) as plotted in Fig. 6.

Shifting the plasma vertically does not result in a 100% transfer of energy from one tile to the next. This is

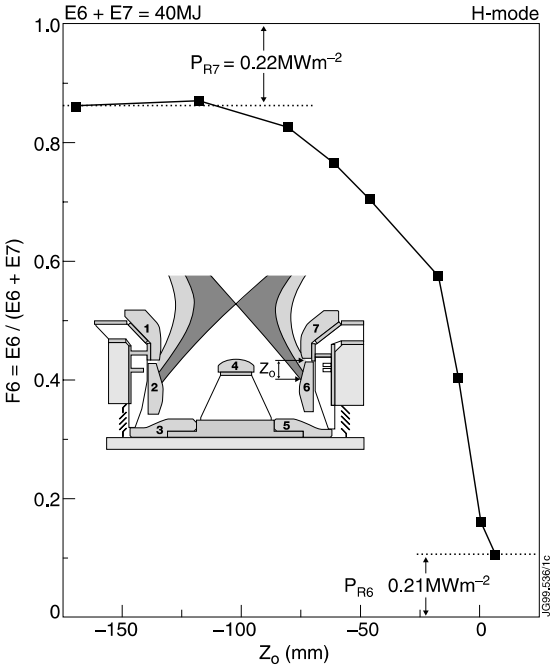

Fig. 6. Fractional energy deposited on outer tile 6 vs vertical displacement of the strike point.

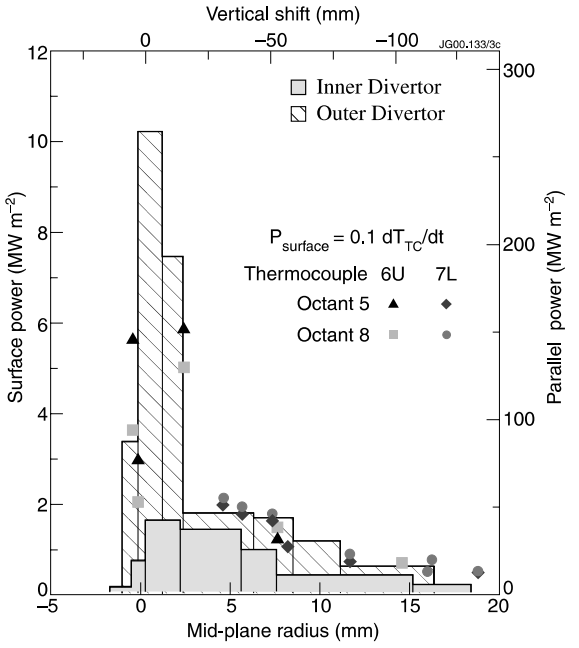

Fig. 7. Power profiles for 12 MW unfuelled H-modes for the inner divertor and outer divertor from pulse-to-pulse shifting are shown as vertical bars ($P \propto dE/dz$). The points are an independent method of determining surface power during the pulse from the time derivative of thermocouple temperature. Results from tile 6 upper thermocouple (6U) and tile 7 lower (7L) are in good agreement.

due to volumetric power losses from electromagnetic radiation and energetic neutrals which are deposited over a large area of the divertor surfaces.

In the case of steady-state discharge the average power density to a vertical surface can be calculated from the derivative of the energy with respect to the strike point displacement:

$$P_{\text{surface}} = \frac{\Delta E}{2\pi R t \Delta Z},$$

where ΔE is the change in tile energy when the strike point is shifted vertically a distance ΔZ, R the major radius of the strike point and t is the duration of the heating pulse. The results of this procedure are plotted in Fig. 7 and reveal a striking narrow peak at the outer target. Apart from this feature the underlying profile is only slightly asymmetric in favour of the outer divertor as one might expect simply from geometric considerations. The approximate (due to variations in flux expansion) parallel power density is also indicated on the right-hand axis.

6. Target probe data and comparison with OSM2/NIMBUS

During the X-point height scan measurements were also made using the target Langmuir probes. They show a similar profile shape with the same narrow feature at the outer strike point as is observed in the thermocouple data. However, the parallel power density calculated from the Langmuir probes assuming equal ion and electron power flow to the SOL is only one quarter of the value derived from the thermocouples. The main contribution to the peak in power seen by the probes is a peak in the ion flux which is ten times higher than the base value. To match the power density determined by the probes with that from the thermocouples you have to assume an ion to electron power ratio of 10 in the 'onion-skin' model OSM2/NIMBUS (see Fig. 3 in [4]). This high power density causes the SOL to become isothermal and the same power peak appears at the inner divertor so a more directional source of power is required. We propose that the narrow peak at the outer target is caused by a kinetic effect, namely ion-orbit loss of fast ions from within the separatrix [5,6] which go predominantly to the outer divertor for the normal direction of the grad **B** drift. Neo-classical fluid drifts may also contribute to the asymmetries but cannot explain the separatrix feature [7].

7. Conclusions

Experiments carried out in MkIIGB have shown the value of divertor thermocouple analysis in diagnosing

the energy and power distributions in the divertor. The results show that there is good energy balance in most discharges and that a substantial part of the ELM energy must be deposited on the divertor target. Power profiles deduced from pulse-by-pulse shifting of the plasma show a narrow (~2 mm mid-plane) high power feature at the outer target which delivers ~50% of the divertor energy and cannot be explained by conventional edge fluid models. The most likely cause of this narrow power peak is ion orbit loss of hot ions from within the separatrix [5,6]. These ions are almost collisionless within the narrow layer [4]. The robustness of the in/out energy asymmetry in JET suggests that this effect is always important. Even when the collisionality of the divertor is high enough to stop these ions from reaching the target, they cannot be ignored since they will have a major impact on the poloidal distribution of the energy and momentum source terms. An important proof of these deductions will be to repeat the experiments with $\mathbf{B} \times \nabla \mathbf{B}$ reversed in which case the lost ion orbits are expected to terminate predominantly at the inner divertor target [6].

References

[1] S. Clement, J. Nucl. Mater. 266–269 (1999) 266.
[2] E. Gauthier, Invited paper, these Proceedings.
[3] L.C. Ingesson, JET-R (99)06.
[4] W. Fundamenski, Contributed paper, these Proceedings.
[5] J. Lingertat, Contributed paper, these Proceedings.
[6] A.V. Chankin, G.M. McCracken, Nucl. Fus. 33 (10) (1993) 1459.
[7] A. Chankin, Invited paper, these Proceedings.